Journal of Scientific & Industrial Research
Vol. 78, April 2019, pp. 223-230

An Entropy-Deng's Similarity-based technique for Modeling and Optimization of Process Variables for Laser Micro Drilling of Alloy-X

Sivaprasad P V[1] and Noorul Haq A[2]*

Department of Production Engineering, National Institute of Technology Tiruchirappalli-620015, Tamilnadu, India

Received 12 April 2018; revised 13 November 2018; accepted 16 February 2019

Laser drilling is a typical process for creating micro holes in hard to cut materials. Though this process is fast, the fickle nature of laser beam often leads to a quality drop in the holes. So, it is vital to analyze the process by developing a higher order model. There is also an urge for achieving the optimal combination of variables to produce the best holes without compromising both productivity and accuracy aspects. This work intends to find out the best laser parameter combination that can yield best holes in an Alloy-X material. Four input factors; power, pulse width, pulse frequency & gas pressure and six possible outputs were considered and evaluated. The relative weights of each output were measured by entropy weight method, and performance index of the response was assessed by Deng's Similarity-based technique. Pulse frequency is found to be the most impact factor, and the gas pressure influences the least. Response Surface Methodology is applied to model the performance index. The metallurgical studies done in the microhole explains the thermal effects during machining.

Keywords: Micro-Drilling, Laser, Entropy Method, Similarity-Based Technique, Alloy-X, Modeling

Introduction

Laser drilling is a process of focusing a high-intensity laser beam onto the workpiece which melts and vaporizes the material to create a hole. Since holes are drilling at the finishing stage, the quality of holes is crucial for the acceptance of a product. The tiny holes are produced by percussion drilling in which the pulsed laser energy repeatedly strikes over the material surface to remove the material layer by layer. One significant laser drilling application is making holes on avionic parts for enhancing the heat transfer[1]. Laser Beam Machining (LBM) is the commonly used technique to produce effusion cooling holes on Ni-based superalloy. Other two prominent methods such as Electro-Chemical Machining (ECM) and Electrical Discharge Machining (EDM) are limited these days due to their adverse environmental impacts and high cost. A laser is also an extensive tool for making complex micro shapes.The accuracy, productivity and the repeatability of microfeatures are the primary concern while machining at the micro level. Therefore, for productive and precise machining, it is necessary to model the process and identify the optimal critical factors for adopting possible controlling measures.

Author for Correspondence
E-mail: anhaq@nitt.edu

Decision-making techniques in machining

Multi-Criteria Decision Making (MCDM) techniques are always useful in finding the best combination, though there is a clash between the criteria. Many of the MCDM methods are frequently using in the machining field. The TOPSIS concept was applied along with the Taguchi and Fuzzy analysis to determine the optimal parameters for EDC process[2]. A blended approach of VIKOR and Entropy weight measurement method was used to optimize the machining parameters of EDM process[3]. GRA is used to assess the best process parameters in conventional micro-drilling of CFRP composites[4]. MOORA method was applied to find the optimal condition in abrasive waterjet process for machining composite[5]. AHP was utilized to prioritize the machining parameters using a pairwise comparison matrix[6]. TOPSIS method is considered as the most used MCDM approach in the manufacturing domain. This concept was advanced based on the notion that the optimal solution will be very much adjacent to the positive ideal solution and that much farther from the negative ideal solution. Though TOPSIS is giving the optimal results, it has been revealed to be impotent to adopt the preference in some cases because the measured distance may create confusion while selecting the best alternative. It was Deng in 2007, who introduced a novel concept; 'Similarity-Based

Approach[7]' to overcome the drawbacks of TOPSIS. In this, the relative similarity between all alternatives and the ideal solution is accounted by the degree of conflict and the similarity between them. The optimal alternative will have the highest degree of similarity towards the positive ideal solution and the lowest degree of similarity towards the negative ideal solution. Comparison studies done between TOPSIS and Similarity-based approach stated that the similarity-based approach had presented a superior ranking outcome[7,8]. Studies were also done with AHP-Deng's similarity approach to realize the optimal wire-EDM process parameters[9].

Apart from that, only limited works were found in the literature regarding the ranking of alternatives based on Deng's similarity-based approach.In general, the weight of each attribute was decided by the decision maker, which creates bias in determining the optimal alternative. So, it is essential to use a standard weight measurement method which resolves the weight of each output response without any favoring decisions. Entropy weight measurement is one such method[3] which calculate the response weight without any prior decisions. This study is dealing with the micro-drilling aspect of a thick Alloy-X material using pulsed Nd:YAG millisecond laser. The best input combination is decided by analyzing the overall performance index (Pi) value obtained from the combination of Entropy and Deng's similarity-based technique. Response Surface Methodology (RSM) is used to model the index 'P_i' to understand how the laser variables impacts on both hole quality and productivity. The surface studies conducted will helps to understand the thermal effects over the drilled zone.

Materials and methods

Material selection

The material Alloy-X is a trademark of Haynes Inc., USA.This material is also known as Hastelloy®-X and Inconel®- HX. It is a solution hardened nickel base superalloy having an austenitic microstructure[10]. The major elemental constituents are Nickel (Ni), Chromium (Cr), Iron (Fe), Molybdenum (Mo), Cobalt (Co), Manganese (Mn) and Tungsten (W). This material has a specific strength and oxidation resistance up to 1200°C. Alloy-X is one of the most prominent metal for making high-temperature gas turbine engine combustion-zone parts such as transition ducts, combustor cans, spray bars and flame holders as well as in the afterburners, tailpipes, and cabin heaters. The corrosion resistance property of this material also makes it suitable for the petrochemical process industry[11].

Experimental plan

Alloy-X sheet is procured from the market and cut into 25mm *x* 21mm *x* 2.0mm size. Before drilling, the cut samples were rinsed in the acetone. JK300D pulsed Nd: YAG milli-second laser machine is used for the experiment.The beam wavelength and spot diameter were 1064nm and 200µm respectively. Nitrogen(N_2)is used as the assist gas. A focal distance of 400µm is fixed while drilling. RSM based rotatable Central Composite Design (CCD) is utilized to design the experimental matrix. The software package Design Expert® Version 7.0 is used for constructing the matrix. The machining variables; Power (P), Pulse width (PW), Pulse repetition rate/ Pulse frequency (PRR) and Gas pressure (GP) were selected based on previous works and practical feasibilities. The ranges of each variable are determined based on pilot experiments. As per CCD, five different input levels were chosen and are coded inbetween -2 to +2 in steps of 1. 'P' varies between 150- 250W, 'PW' is selected in the range of 0.1- 0.5ms, 'PRR' varies in the scale of 100 - 140Hz and 'GP' is controlled in between 8-12bar. The outputs evaluated for a micro hole are Material Removal Rate (mm^3/min [MRR]), Entrance Diameter (mm, [D_t]), Exit Diameter (mm, [D_b]), Taper (mm/mm, [α]), Entrance circularity error (mm, [ε_t]), and Exit circularity error (mm, [ε_b]). 'MRR' indicates the productivity of the process. It is the ratio of the weight differences (Δw) of the sample before and after the machining to the density (ρ) of the material.The density of the procured material is found out as $8.13\ \mathrm{gm/cm^3}$.'Taper'exists in a laser drilled hole because of the converging-diverging nature of the laser beam[12]. The evaluation of Taper discursively defines the amount of cylindricity that a hole bears. Taper defined as the ratio of the difference in both end diameters ($\Delta D = D_T - D_B$) to the depth of drilling (d).All other features such as diameters and the circularity errors were measured with the help of a Video Measuring Machine (VMM). The machine was manufactured byARCS Precision Technology Co. Ltd., Taiwan, ROC. The setup has a least count value of 1µm and an accuracy of 4µm. The diameters and circularity errors were measured in 'mm.' Multiple

measurements were taken from each sample, and the average value is considered for modeling.

Entropy weight method

The weights of each attribute are critical in determining the overall performance index. The steps included in the entropy weight measurement approach are describing as follows[8]: Convert the input variables and the outputs into *'m'* alternatives and *'n'*attributes respectively, Develop a Decision matrix, $D[x_{ij}]_{m\ x\ n}$consists of the results obtained after experiments; The order of the matrix should be $m \times n$. where, 'm' accounts the total number of experiments and 'n' is considered as the total responses. $'x_{ij}'$ denotes the outcome of the j^{th} response for the i^{th}experiment; Normalize the matrix $[D]$ with general maximization and minimization criteria. The normalized matrix will be denoted as 'r_{ij}' Obtain the matrix T = $(T_{ij})_{m\ x\ n}$ by dividing each components of matrix 'r_{ij}; with its individual total sum value ($\sum_{i=1}^{m}(r_{ij})$).

Measure the entropy weight $'w_j'$ for the j^{th}response.

$$w_j \ \frac{1+(\frac{1}{\ln m}[\sum_{i=1}^{m} T_{ij} \ln(T_{ij})])}{n-\sum_{j=1}^{n}(\frac{1}{\ln m}[\sum_{i=1}^{m} T_{ij} \ln(T_{ij})])} \quad \ldots (1)$$

Represent the weightage of all responses in a weighting vector *'W'*

Deng's similarity based technique

After obtaining the weight for each response, Deng's similarity- based method is applied to find the best alternative among the set of the designed experimental matrix. The step by step procedure for this method is explained below[7].

- Determine the normalized decision matrix X.
- Assign the individual weights (obtained from Entropy method) for each response.
- Find the weighted performance matrix *'Y'* by multiplying the normalized decision matrix X with weighting vector *'W'*. This matrix shows the performance of each alternative concerning each criterion.
- Calculate the Positive Ideal Solution (PIS) and Negative Ideal Solution (NIS).
- Estimate the degree of conflict ($cos\Theta_i^{\pm}$)among each alternative $'A_i'$ and PIS & NIS.
- Obtain the degree of similarity ($S_i^{\pm}$) between$'A_i'$ and the PIS & NIS.The similarity value is the ratio between $|C_i|^{\pm}$ to $|A|^{\pm}$. Where, $|C_i|^{\pm}$ is the product output between degree of conflict and square root of the total sum of the square of the weighted performance matrix. Also, $|A|^{\pm}$ is the square root value of the total sum of the square of the ideal solutions[9].

  Measure the Overall Performance Index (P_i)

$$P_i = \frac{S_i^{+}}{S_i^{+} + S_i^{-}} \quad \ldots (2)$$

Larger the P_i value implies the most desirable alternative.

Rank the m number of alternatives in the descending order of their P_i value.

Response surface methodology (RSM)

RSM is a fractional factorial design which used to create and conduct the experiments. In comparison to other fractional factorial methods, RSM provides a much accurate prediction of results especially in predicting the primary and interaction term's effects on the responses. The output is represented as a surface which is explained by a higher order equation as given below [13],

$$Y = \beta_0 + \sum_{i=1}^{k} \beta_i X_i + \sum_{i=1}^{k} \beta_{ii} {X_i}^2 + \sum\sum_{i<j} \beta_{ij} X_i X_j \pm \varepsilon$$

here Y is the output response. The symbols $\beta_0, \beta_i, \beta_{ii}$and β_{ij} are the coefficient values of the obtained model. The symbols$X_i, {X_i}^2$ and $X_i X_j$ are the linear, quadratic, and two-factor interaction terms respectively. The symbol 'i' displays the number of input variables considered and the symbol'ε' is the possible error in the fitted curve equation.

Results and Discussion

The 'decision matrix' is the 'response matrix' shown in Table 1. The subsequent steps of the Entropy weight approach and Dengs similarity approach are presented in Table 2. The table shows the significant values obtained from Entropy as well as the Dengs method. The weight of each response is calculated using Equation1. The weighting vector (W) representing the weights of each response is given below,

'W'= (MRR, D_t, D_b, α, ε_t, ε_b) = (0.39723, 0.12098, 0.15964, 0.08603, 0.12259, 0.11353)

MRR is having the highest weightage, followed by exit diameter, entrance circularity error, entrance diameter, exit circularity error, and the taper.From

Table 1 — Thirty run CCD experimental matrix with response values

Exp. No.	Input Parameters				Response Matrix					
	P	PW	PRR	G P	MRR	D_t	D_b	α	ε_t	ε_b
1	200	0.3	120	10	0.00387	0.285	0.230	0.0220	0.02885	0.02418
2	200	0.5	120	10	0.02148	0.363	0.332	0.0124	0.03770	0.02180
3	225	0.4	110	9	0.02689	0.394	0.252	0.0568	0.03489	0.00948
4	200	0.3	120	10	0.00549	0.273	0.232	0.0164	0.02970	0.02700
5	175	0.2	110	9	0.01065	0.265	0.195	0.0280	0.00297	0.00942
6	200	0.3	120	8	0.01361	0.452	0.245	0.0828	0.03000	0.01450
7	200	0.3	140	10	0.00032	0.265	0.262	0.0012	0.02000	0.01754
8	200	0.3	120	12	0.01435	0.288	0.218	0.0280	0.02700	0.01898
9	150	0.3	120	10	0.01835	0.218	0.198	0.0080	0.01760	0.01300
10	225	0.4	130	9	0.01557	0.393	0.325	0.0272	0.04901	0.03381
11	200	0.3	120	10	0.00501	0.285	0.225	0.0240	0.02150	0.02754
12	225	0.2	110	9	0.01171	0.357	0.233	0.0496	0.02916	0.00614
13	175	0.2	110	11	0.00729	0.265	0.252	0.0052	0.00928	0.00481
14	200	0.3	100	10	0.01466	0.323	0.268	0.0220	0.00250	0.00139
15	225	0.4	130	11	0.02425	0.265	0.254	0.0044	0.05012	0.04691
16	175	0.2	130	9	0.00240	0.251	0.240	0.0044	0.01290	0.00508
17	175	0.2	130	11	0.00096	0.232	0.190	0.0168	0.01998	0.00378
18	175	0.4	130	11	0.00508	0.284	0.251	0.0132	0.02819	0.01818
19	175	0.4	130	9	0.00663	0.392	0.321	0.0284	0.01813	0.01389
20	225	0.4	110	11	0.03413	0.305	0.283	0.0088	0.03854	0.01568
21	200	0.3	120	10	0.00726	0.295	0.240	0.0220	0.02896	0.02514
22	250	0.3	120	10	0.03552	0.335	0.237	0.0392	0.06000	0.03600
23	200	0.3	120	10	0.00700	0.297	0.213	0.0336	0.02895	0.02700
24	200	0.1	120	10	0.00176	0.265	0.247	0.0072	0.01560	0.00200
25	200	0.3	120	10	0.00589	0.268	0.223	0.0180	0.02938	0.02612
26	225	0.2	110	11	0.01000	0.340	0.293	0.0188	0.02548	0.01145
27	225	0.2	130	9	0.00848	0.312	0.272	0.0160	0.02819	0.01695
28	175	0.4	110	9	0.02495	0.375	0.239	0.0544	0.01389	0.00582
29	225	0.2	130	11	0.01046	0.270	0.230	0.0160	0.03215	0.02018
30	175	0.4	110	11	0.01854	0.299	0.262	0.0148	0.01233	0.00814

Table 2; it is inferred that the highest index value belongs to the twentieth experiment, which is the most desirable factor level combination.

The corresponding parameter combinations are: $[\mathrm{P}, \mathrm{PW}, \mathrm{PRR}, \mathrm{GP}] = [225, 0.4, 110, 11]$.

It is also significant to find out the effects of different machining parameter's impacts on the index. This can be done by modeling the index using statistical techniques. RSM is used to develop a quadratic model to explain the effects of the laser variables on the performance index. Design Expert® Version 7.0 is used as a platform to construct the regression model, and ANOVA analysis is used to check the adequacy of the model.Equation 3 is the model developed based on RSM concept. The input variables are at their coded levels.

$$\mathrm{P_i} = 0.27 + 0.018\ (\mathrm{P}) + 0.065\ (\mathrm{PW}) - 0.1\ (\mathrm{PRR}) + 0.00853\ (\mathrm{GP}) + 0.00613\ (\mathrm{P\ x\ PW}) + 0.049\ (\mathrm{P\ x\ PRR}) + 0.027\ (\mathrm{P\ x\ GP}) - 0.021\ (\mathrm{PW\ x\ PRR}) + 0.018\ (\mathrm{PW\ x\ GP}) - 0.0015\ (\mathrm{PRR\ x\ GP}) + 0.079\ (\mathrm{P^2}) + 0.024\ (\mathrm{PW^2}) + 0.018\ (\mathrm{PRR^2}) + 0.038\ (\mathrm{GP^2}) \quad \ldots (3)$$

The equation shows that power, pulse width, and the assist gas pressure have a positive effect on the performance index and the repetition rate has a negative impact as well. Table 3 indicates the individual, interactive and higher order parameter's effect on the index.

Table.2 - Combined tabulated results of the Entropy Weight Method and the Deng's Similarity Based Approach

	Tabulated results of the Entropy Weight Method						Tabulated results of the Deng's Similarity Based Approach							
Exp. No.	$T_{ij}\ x\ ln(T_{ij})$ Matrix						Degree of Conflicts between alternatives				The Similarity and Performance values of alternatives			
	MRR	D_t	D_b	α	ε_t	ε_b	$\cos\theta^+$	$\cos\theta^-$	C_i^+	C_i^-	S^+	S^-	P_i	Ranking
1	-0.0452	-0.1252	-0.1306	-0.1151	-0.1068	-0.0933	0.4567	0.9062	0.0237	0.0470	0.1409	0.4979	0.2205	28
2	-0.1657	-0.0796	0.0000	-0.1275	-0.0838	-0.1002	0.9176	0.4689	0.1071	0.0547	0.6365	0.5793	0.5235	08
3	-0.1914	-0.0576	-0.1102	-0.0616	-0.0914	-0.1327	0.9458	0.4024	0.1310	0.0557	0.7785	0.5900	0.5689	06
4	-0.0606	-0.1313	-0.1288	-0.1225	-0.1047	-0.0846	0.5578	0.8470	0.0312	0.0473	0.1853	0.5012	0.2699	24
5	-0.1013	-0.1353	-0.1592	-0.1070	-0.1615	-0.1329	0.8918	0.4864	0.0540	0.0295	0.3210	0.3119	0.5072	09
6	-0.1211	0.0000	-0.1169	0.0000	-0.1039	-0.1201	0.7551	0.6806	0.0700	0.0631	0.4162	0.6682	0.3838	17
7	0.0000	-0.1353	-0.1002	-0.1411	-0.1273	-0.1121	0.1754	0.8341	0.0075	0.0358	0.0447	0.3788	0.1056	30
8	-0.1258	-0.1236	-0.1409	-0.1069	-0.1112	-0.1082	0.8851	0.5592	0.0719	0.0454	0.4271	0.4807	0.4705	11
9	-0.1491	-0.1572	-0.1569	-0.1330	-0.1325	-0.1240	0.9692	0.3404	0.0894	0.0314	0.5313	0.3324	0.6151	02
10	-0.1332	-0.0583	-0.0165	-0.1081	-0.0489	-0.0618	0.7882	0.6779	0.0801	0.0689	0.4762	0.7296	0.3949	16
11	-0.0562	-0.1252	-0.1349	-0.1125	-0.1239	-0.0829	0.5384	0.8649	0.0289	0.0464	0.1716	0.4909	0.2590	26
12	-0.1086	-0.0835	-0.1279	-0.0741	-0.1060	-0.1407	0.8050	0.6284	0.0603	0.0471	0.3586	0.4987	0.4183	13
13	-0.0759	-0.1353	-0.1102	-0.1363	-0.1495	-0.1437	0.7941	0.5281	0.0393	0.0262	0.2338	0.2769	0.4578	12
14	-0.1276	-0.1044	-0.0939	-0.1151	-0.1624	-0.1515	0.9287	0.3609	0.0739	0.0287	0.4394	0.3042	0.5909	05
15	-0.1793	-0.1353	-0.1082	-0.1373	-0.0450	0.0000	0.8850	0.4835	0.1183	0.0646	0.7034	0.6845	0.5068	10
16	-0.0295	-0.1421	-0.1216	-0.1373	-0.1423	-0.1431	0.4495	0.7129	0.0165	0.0262	0.0981	0.2772	0.2614	25
17	-0.0111	-0.1509	-0.163	-0.1219	-0.1273	-0.1461	0.2719	0.8514	0.0091	0.0283	0.0538	0.3001	0.1520	29
18	-0.0569	-0.1257	-0.1112	-0.1265	-0.1084	-0.1103	0.5702	0.8200	0.0295	0.0425	0.1756	0.4499	0.2808	23
19	-0.0704	-0.0590	-0.0239	-0.1064	-0.1313	-0.1217	0.6264	0.7565	0.0383	0.0463	0.2279	0.4904	0.3173	19
20	-0.2211	-0.1145	-0.0771	-0.1320	-0.0814	-0.1170	0.9788	0.2870	0.1642	0.0482	0.9762	0.5099	0.6569	01
21	-0.0756	-0.1199	-0.1216	-0.1151	-0.1065	-0.0903	0.6538	0.8019	0.0396	0.0485	0.2352	0.5139	0.3140	20
22	-0.2263	-0.0973	-0.1243	-0.0907	0.0000	-0.0537	0.9416	0.4035	0.1706	0.0731	1.0140	0.7741	0.5671	07
23	-0.0735	-0.1188	-0.1450	-0.0990	-0.1065	-0.0846	0.6243	0.8399	0.0380	0.0512	0.2260	0.5417	0.2944	21
24	-0.0219	-0.1353	-0.1150	-0.1339	-0.1367	-0.1501	0.3675	0.7179	0.0138	0.0269	0.0819	0.2849	0.2232	27
25	-0.0641	-0.1338	-0.1367	-0.1204	-0.1055	-0.0874	0.5886	0.8366	0.0328	0.0466	0.1951	0.4939	0.2831	22
26	-0.0967	-0.0942	-0.0649	-0.1194	-0.1148	-0.1279	0.7887	0.6388	0.0532	0.0431	0.3161	0.4560	0.4094	14
27	-0.0853	-0.1106	-0.0896	-0.1230	-0.1084	-0.1137	0.7317	0.7121	0.0457	0.0445	0.2716	0.4709	0.3658	18
28	-0.1826	-0.0714	-0.1225	-0.0659	-0.1403	-0.1414	0.9581	0.3477	0.1215	0.0441	0.7222	0.4669	0.6073	03
29	-0.0999	-0.1328	-0.1306	-0.1230	-0.0985	-0.1048	0.7978	0.6618	0.0540	0.0448	0.3210	0.4743	0.4036	15
30	-0.1502	-0.1178	-0.1002	-0.1245	-0.1434	-0.1359	0.9607	0.3517	0.0917	0.0336	0.5451	0.3555	0.6053	04

Pulse repetition rate (PRR) is the most significant factor followed by the square term of power (P), independent term Pulse width (PW), the squared term of gas pressure (GP), the interaction term of P & PRR, and so on. The R^2_{Pred} value of 80% indicates the fitness of the model. Figure 1 illustrates the compactness of the predicted data with the actual data.

Three-dimensional contour plot has been generated by keeping the major individual factors (PRR & PW) on the X & Y axis and the other two variables (P & GP) in their coded mean level (0). The graph which

has plotted using the software package Matlab® 2016b is shown in Figure 2.

The significant findings from the ANOVA & Contour graphs are as follows;

- The index(P_i) value is increased with an increase in pulse width. This is because an increase in pulse width enhances the fluence value at the laser striking surface. This improves the MRR and the diameters of the hole.
- An increase in frequency reduces the P_i value. At medium power, if the frequency increases, the pulse off time will be minimized, which results in a low energy beam striking at the machine surface, results in low MRR. Also, at the high-frequency condition, the time taken to solidify the molten metal at the fringes of the hole are limited which causes derangement in the drilling process, results in circularity error.This condition also increases the spatter area and spatter thickness around the hole periphery.
- Power is having the highest interaction impact on P_i with other variables. The interaction between power and frequency is comparatively higher. A low value of power along with an increase in frequency causes enlargement in exit diameter and reduces taper. Whereas, high power value along with high-frequency ranges removes material from the top surface and increases the taper. A high level of gas pressure along with

Table 3 — ANOVA of the P_i value

Factor	Sum of squares	*F*-Value	*p*-Value	% Contribution
Model	0.63	24.78	< 0.0001	95.455
P	0.00804	4.41	0.053	1.2185
PW	0.1	55.89	< 0.0001	15.152
PRR	0.26	145.12	< 0.0001	39.394
GP	0.00175	0.96	0.3432	0.2644
P x PW	0.000602	0.33	0.574	0.0912
P x PRR	0.038	21.08	0.0004	5.7576
P x GP	0.011	6.23	0.0247	1.6667
PW x PRR	0.00676	3.71	0.0733	1.0239
PW x GP	0.0053	2.91	0.1086	0.8035
PRR x GP	0.000036	0.02	0.8904	0.0054
P^2	0.17	93.79	< 0.0001	25.758
PW^2	0.016	9.03	0.0089	2.4242
PRR^2	0.0091	4.99	0.0411	1.3780
GP^2	0.039	21.67	0.0003	5.9091

$R^2 = 0.95$ $R^2_{adj} = 0.92$ $R^2_{Pred} = 0.80$

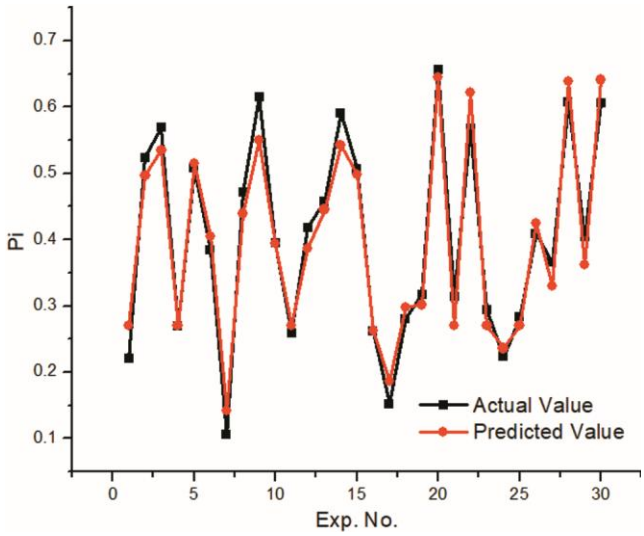

Fig. 1 — Similarity plot between actual and predicted P_i

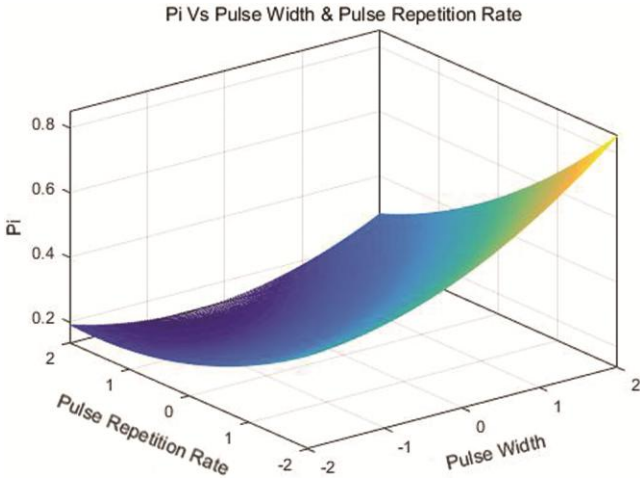

Fig. 2 — Contour graph showing the effect of pulse width and frequency on P_i at the mean level of power and gas pressure

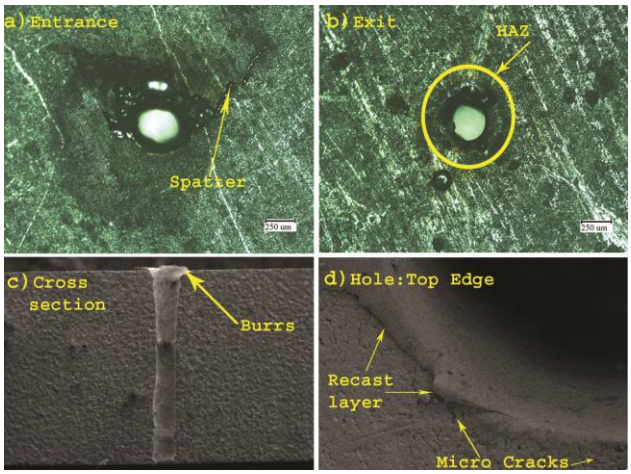

Fig. 3 — Hole entrance and exit at optimal parametric conditions, micro-cracks near the hole brink and cross-section of the micro hole

power induces a chilling effect on the machined regime and boosts the solidification of molten metal to reduces the diameter enlargement. Thus, the taper will minimize.

- Proper assist gas pressure removes the debris and reduces the churning of the molten metal to maintains the accuracy of the hole. Increase in workpiece thickness will reduce the effect of assist gas.In this study, the workpiece used is comparatively thicker. Hence, the impact of gas pressure is negligible.

Hole surface characteristics

LBM process produces typical thermal effects such as Heat Affected Zones (HAZ) and spatters[14]. Fast heating and cooling property of laser also lead to recast layers (RL) in drilled holes[15]. The same phenomenon also causes microcracks near the hole fringe and alters the behavior of the surface.Figure 3 showing the optical microscope (OM) image of the hole drilled at best factor level combination at 500X magnification. A Scanning Electron Microscope (SEM) images of the edge and the cross section of the micro hole are also given. Glyceregia solution is used for etching the hole sections. The solution is a combination of hydrochloric acid (HCl), glycerol ($C_3H_8O_3$) and nitric acid (HNO_3) in the ratio of 3:2:1. The hole section consists of spatters and thermal affected zones. Spatters are the results of the solidification of metal around the drilled surface due to the improper removal of the molten material. The HAZ is visible around the hole brink. The SEM image shows the presence of microcracks and recast layer near the hole edges. These are due to the existence of thermal gradient during drilling. This gradient can be minimized by proper use of assist gas. The cracks and the heat affected zones were also influenced by pulse duration and the pulse frequency. The SEM image of the hole edge was captured at 250X magnification, and the cross-section of the drilled hole is taken at 30X magnification. The top side is widened a little due to the prolonged exposure of the surface with the laser beam, which leads to over melting of the top surface results in an enlargement of the top edge.

Conclusions

Laser beam machining is the most used micro-drilling technique for materials useful for extreme applications. Alloy-X is a potential superalloy used in the aeronautics and petrochemical industries for high temperature and corrosive environment applications. For general cooling purposes, micro holes are drilling to the parts made from this material. The Entropy-Deng's combined method is found as suitable to identify the best laser machine input combination to drill an optimal micro-hole in Alloy-X. The Entropy analysis founds that; productivity has the higher weightage followed by the accuracy terms. The ANOVA analysis reveals the critical input variables that were influencing the overall performance index (P_i). Pulse repetition rate is the most dominant factor followed by pulse width. Both power and gas pressure hold the highest interaction and square effects respectively. The Surface integrity analysis reveals that the drilled hole contains microcracks, recast layers, spatters,burrs, and HAZs. The proper use of assist gas can cut down the micro-cracking tendencies with its cooling property. Though LBM is the best process for superalloy machining in terms of speed, it retains some severe drawbacks concerning accuracy and surface integrity. This could be controlled or eliminated by applying different sequential (hybrid) machining combinations.

References

1 Jain V K, Sidpara A, Balasubramaniam R, Lodha G S, Dhamgaye V P & Shukla R, Micromanufacturing: a review—part I, *Proc Inst Mech Eng, Part B: J EngManuf*, 228(2014) 973-994.

2 Chakraborty S, Kar S, Dey V& Ghosh S K, Multi Attribute Decision Making for Determining Optimum Process Parameter in EDC with Si and Cu Mixed Powder Green Compact Electrodes, *J Sci Ind Res*, 77(2018) 229-236.

3 Bhuyan R & Routara B, Optimization the machining parameters by using VIKOR and Entropy Weight method during EDM process of Al–18% SiCp Metal matrix composite, *Decis Sci Lett*, 5(2016) 269-282.

4 Shunmugesh K &Panneerselvam K, Optimization of Process Parameters in Micro-drilling of Carbon Fiber Reinforced Polymer (CFRP) Using Taguchi and Grey Relational Analysis, *Polym&Polym Compos*, 24(2016) 499.

5 Kalirasu S, Rajini N, Rajesh S, WinowlinJappes JT &Karuppasamy K, AWJM Performance of jute/polyester composite using MOORA and analytical models, *Mater Manuf Processes*32 (2017) 1730-1739.

6 Kalpande S D &Badgujar P, Investigation of abrasive water jet cutting quality process parameter by AHP method, *Int J Manage Enterp Dev*, 14(2015) 242-249.

7 Deng H, A similarity-based approach to ranking multicriteria alternatives, in *Int ConfIntellComput* (Springer, Berlin) 253-262 August 2007.

8 Sonkar V, Abhishek K, Datta S & Mahapatra S S, Multi-objective optimization in drilling of GFRP composites: a degree of similarity approach, *Procedia Mater Sci*, 6 (2014) 538-543.

9 Babu K A, Venkataramaiah P & Dileep P, AHP-DENG'S Similarity Based Optimization of WEDM Process Parameters of Al/SiCp Composite. *Am J Mater Sci Technol*, 6(2017) 1-14.

10 Pakniat M, Ghaini F M & Torkamany M J, Hot cracking in laser welding of Hastelloy X with pulsed Nd: YAG and continuous wave fiber lasers, *Mater Des*, 106(2016) 177-183.

11 Marchese G, Basile G, Bassini E, Aversa A, Lombardi M, Ugues D, Fino P &Biamino S, Study of the Microstructure and Cracking Mechanisms of Hastelloy X Produced by Laser Powder Bed Fusion, *Mater*,11(2018) 106.

12 Biswas R, Kuar A S & Mitra S, Process optimization in Nd: YAG laser microdrilling of alumina–aluminium interpenetrating phase composite, *J Mater Res Technol*, 4(2015) 323-332.

13 Montgomery D C, *Design and analysis of experiments* (John Wiley & Sons) 2017.

14 Al-Ahmari A M A, Rasheed M S, Mohammed M K & Saleh T, A hybrid machining process combining Micro-EDM and laser beam machining of Nickel–Titanium-Based shape memory alloy, *Mater Manuf Processes*, 31(2016) 447- 455.

15 Imran M, Mativenga P T, Gholinia A & Withers P J, Assessment of surface integrity of Ni superalloy after electrical-discharge, laser and mechanical micro-drilling processes,*Int J Adv Manuf Technol*, 79(2015) 1303-1311.